Mansoura Engineering Journal, (MEJ), Vol. 29, No. 4, December 2004. M. 38

Effect of Flow Bypass on the Performance of a Shrouded Longitudinal Fin Array

تأثير السريان التجنيبي على أداء مصفوفة زعانف طولية مغطاة

E. A. M. Elshafei
Mechanical Power Eng. Dept. Mansoura University, Mansoura, Egypt
Eelshafei@mans.edu.eg

ملخص البحث

يتناول البحث دراسة نظرية ومعملية لبيان تأثير كل من سرعة الهواء والخلوص بين حافة الزعانف والغطاء الممثل بالسطح العلوي للمجرى الهوائي المثبت به مصفوفة زعانف طولية من الألمنيوم على معامل إمرار الهواء وكذلك على فقد الضغط عبر المصفوفة والأداء الحراري لها. امتدت الدراسة النظرية لتشمل تأثير كثافة الزعانف على معامل إمرار الهواء وفقد الضغط عبر المصفوفة. أجريت الدراسة المعملية على المصفوفة المكونة من سبع زعانف بدون ترك خلوص بين الحافة العليا للمصفوفة والسطح العلوي للمجرى وكذلك في حالة التحديد الجزئي للمصفوفة بتغير ارتفاع المجرى الهوائي ليعطى نسب خلوص (C/H_f) مختلفة. وأثناء التجارب تم تغير نسبة الخلوص من 0.22 حتى 0.89 ورقم رينولدز من 3000 وحتى 38000 . أظهرت النتائج النظرية زيادة معامل الامرار للهواء مع زيادة كثافة الزعانف وأيضا مع زيادة نسبة الخلوص وأن تأثير كثافة الزعانف عليه يقل بزيادة نسبة الخلوص، بينما تبقى قيمه ثابتة تقريبا مع تغير معدل سريان الهواء. تمت مقارنة قيم فقد الضغط المحسوبة عبر المصفوفة بكثافة زعانف مختلفة في حالتي عدم وجود خلوص ووجوده، وقد تبين زيادة مفاقيد الضغط للمصفوفة في حالة عدم وجود خلوص لنسب $H_f/S = 8$ & 12.75 بمعامل $4.3, 20$ على التوالي مقارنة بتلك التي لها نسبة $H_f/S=3.4$ وأن هذا التأثير يقل بزيادة الخلوص. وبمقارنة النتائج المعملية على المصفوفة التي تحوى 7 زعانف $(H_f/S=3.4)$ لفقد الضغط عبرها وكذلك معاملات انتقال الحرارة بالحمل بين ريش المصفوفة والهواء في حالتي عدم وجود خلوص ووجوده بنسب مختلفة ، وجد أن فقد الضغط لنسبة خلوص 0.89 يقل إلى حوالي 50% من قيمته في حالة عدم وجود خلوص وأن معاملات انتقال الحرارة تقل عند قيمة رقم رينولدز حوالي 3000 بنسب 12, 17, 30% لنسب خلوص0.89 ,0.56 ,0.36 على التوالي مقارنة بحالة عدم وجود خلوص ، وأن نسب الانخفاض هذه في معاملات انتقال الحرارة بالحمل تقل مع زيادة معدل سريان الهواء.

Abstract

Theoretical and experimental studies were carried out to investigate the effects of duct velocity, fin density and tip-to-shroud clearance on the flow bypass and its impact on the pressure drop across a longitudinal aluminum fin array and its thermal performance. The clearance was varied parametrically, stating with the fully shrouded case and variations of the channel height giving partially shrouded configuration of different clearance ratios were also carried out. The flow bypass was found to increase with increasing fin density and insensitive to the air flow rate. That effect of fin density decreased as the clearance increased. The calculated total pressure was greatly affected by fin density. For fully-shrouded fin array, with H_f/S equals to 8 and 12.72, the pressure drop increased by a factor of 4.3 and 20 of that with H_f/S equals to 3.4, respectively. The total pressure drop and the average convective heat transfer coefficients corresponding to the fully and partially shrouded fin array of $H_f/S=3.4$ were compared. Going from fully to partially shrouded one of the largest clearance ratio ($C/H_f=0.89$), the total pressure drop reduced by about 50%. For clearance ratios equal to 0.36, 0.56, and 0.89, the average heat transfer coefficients were reduced by about 12, 17, and 30 percent of those for the fully shrouded configuration at Re_D of about 3×10^3. That percentage reduction in heat transfer coefficients decreased with the increase of air flow rate.

Keywords; Forced convection; Fin arrays; Cooling of electronic equipment;

Accepted December 30, 2004.

Nomenclature

A area, m^2
BF bypass factor
D_h hydraulic diameter, mm
f friction coefficient, dimensionless
h heat transfer coefficient, W/m^2 K
H height, mm
k thermal conductivity, W/m K
K_{en} entrance loss coefficient
K_{ex} exit loss coefficient
L longitudinal length, mm
m parameter, equation (21)
N_f number of fins
Nu Nusselt number, dimensionless
P pressure, N/m^2
p perimeter, mm
Q rate of heat transfer, W
Re Reynolds number, dimensionless
S fin spacing, mm
T temperature, K
t thickness, mm
V volumetric flow rate, m^3/s
v velocity, m/s
W base plate and fin array width, mm

Greek Symbols

ε Surface roughness, mm
η_f fin efficiency, dimensionless
ν kinematic viscosity, m^2/s
ρ density, kg/m^3
Δ difference

Subscripts

a air
av average
B by pass
bp base plate
D duct
en entrance
ex exit
exp experimental
F free flow
Fr frontal
f fin
fe fin effective
fp fin passage
in input
L loss
pr predicted
s surface
t total
∞ bulk

Introduction

Increasing power density of electronic equipment are requiring more effective thermal enhancement to maintain its operating temperatures at a satisfactory level. Despite its relatively poor thermal properties, air through the use of extended surfaces continuous to be used as a coolant for many electronic devices. Design of such surfaces takes the form of longitudinal fin arrays. If the air velocity through the gaps between fins is well approximated, the thermal performance of such fin arrays and pressure drop across them can be detected. Approximating the fin velocity based on the upstream flow rate in the enclosure is difficult, unless the fin array is fully shrouded, which is not practical. In ducting fin arrays, the approach flow redistribute itself and at least a portion of it will take the path of least resistance and bypass the fin array. The performance of such fin arrays is adversely affected by this flow bypass.

Recently, the studies on heat sink design for forced convection have been conducted. Bejan and Sciubba [1992] have predicted the optimal fin spacing for maximum heat transfer from a package of parallel plates that is cooled by forced convection. Knight et al [1992] have developed fin optimization method for heat sink with micro channels by iterative solution of nonlinear equations for Reynolds number, friction factor, Nusselt number, fin length, and pumping power. Since the surrounding flow field of fin arrays is actually bypass flow over fins, bypass effect should be taken into account.

The effect of flow bypass on the performance of longitudinal fin arrays has been reported by several workers. Sparrow et al [1978], Sparrow and Beckley [1981], and Sparrow and Kadle [1986] investigated the effect of tip clearance on thermal performance of longitudinal plate

fin heat sink. It is reported that the ratio of heat transfer coefficient with and without clearance, to be strongly affected by the tip clearance to fin height ratio, and to be independent of air flow rate and fin height. Experimental results of Butterbaugh and Kang [1995] showed that the thermal resistance is strongly correlated with the pressure drop across the heat sink, and appearing to be independent of the amount of bypass.

Writz et al [1994] studied the effects of flow bypass on the performance of longitudinal heat sinks in ducted flow. It is reported that the values of flow bypass was found up to 60% and its effect was to reduce the overall heat transfer rate. Their study also showed that the design of fin arrays can be optimized for a given flow conditions and shroud configuration. Lee [1995] has analyzed the relationship between the fin geometry and the pressure drop across the fin array taking into account flow bypass from the hydrodynamic analysis and developed an analytical model for optimizing the thermal performance of longitudinal fin arrays in ducted flow.

Thermal characteristics of straight channel longitudinal fin heat sink under forced air cooling were experimentally and numerically investigated using CFD code by Adam and Izundu [1997]. It is reported that much of the augmentation in the heat transfer rates with the heat sink is due to the increased surface area. However, as observed by Writz et al [1994], much of the gain in overall heat transfer rate is offset by the reduction in heat transfer coefficients due to the flow bypass effect which was more pronounced at lower approach flow rates.

Suzana et al [2000] investigated the effects of fin density, air flow rate, and clearance area ratio on flow bypass and its impact on the thermal performance of the heat sink using CFD software. It is concluded that the flow bypass is increased with the increasing fin density and clearance, while remaining insensitive to inlet duct velocity.

Azar and Tavassoli [2003] studied the effect of heat sink dimensions and the number of fins on its thermal performance. It is reported that the selection of heat sink depends not only on its thermal resistance, but also on the number of fins it has and how it is coupled to the board. Simons [2004] has estimated the air flow that actually passes through the fin passages of a ducted heat sink in the presence of flow bypass and investigated the effect of this flow bypass on its thermal performance. It is reported that the flow bypass has a substantial effect on thermal performance of heat sink, and that effect can significantly increase its thermal resistance as the number of fins increases.

Most of the experimental data collected from the previous studies in the above literature did not take the air flow leakage as well as the distribution of air flow through the duct into consideration. An adequate characterization of the thermal performance of such arrays requires a vast amount of data. More experimental work on them and with varying flow regimes is needed. The aim of the present study is to analytically and experimentally investigate the effect of air flow rate, fin density and tip-to-shroud clearance on flow bypass and its impact on the performance of a ducted longitudinal fin array.

Experimental Investigations

Experimental setup

A wind tunnel is used to investigate the performance of the tested fin array. A schematic of this experimental setup is shown in Fig. 1. It mainly consists of the test section, the power supplies, the flow rate, pressure and temperature measurement devices, a control gate, and the fan. An entry length for the tunnel is

made from wood with enough length to assure a uniform flow upstream of the test section for inlet velocities ranging from 1m/s up to 20 m/s.

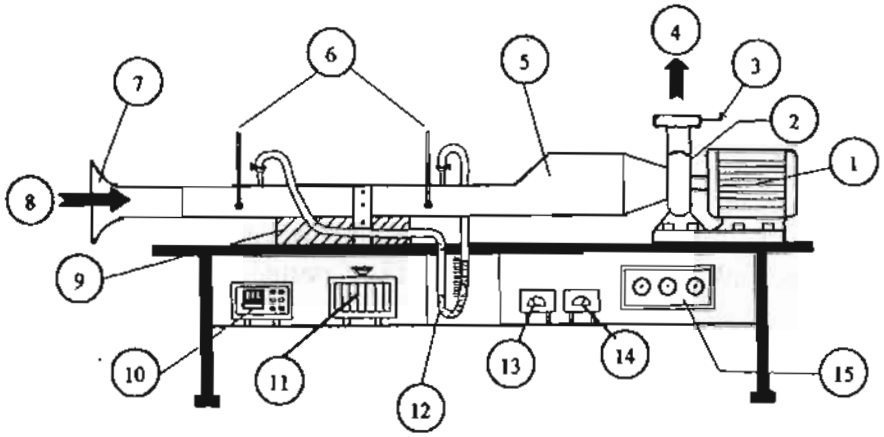

Fig.1. Test Rig

1- Electric motor, 2- Suction air blower, 3- Air flow control gate, 4- Air stream out, 5- Wooden duct, 6- Temperature probes, 7- Bell mouth, 8- Air in, 9- Test section, 10- Digital temperature recorder, 11-Autotransformer, 12- Manometer, 13- Voltmeter, 14- Ammeter, 15- Blower switchboard.

Test Section Components and Configurations

For easy description of the experimental apparatus, reference may be made to Fig. 2, which shows a view of the test section and a cross section of the ducted fin array assembly used in carrying out the experiments when fully shrouded. The wooden test section dimensions of 500×107mm with adjustable top allow accommodating the tested fin array. It includes an array of seven parallel longitudinal fins, a heated base plate, and a wooden shroud with adjustable top that can be moved up and down to change the amount of clearance between itself and the fin tips. The entire array can be easily mounted among the test section with the assurance of good thermal contact and to expose the fins to a nearly uniform air flow as can be reviewed in Elshafei and El-Negiry [2003].

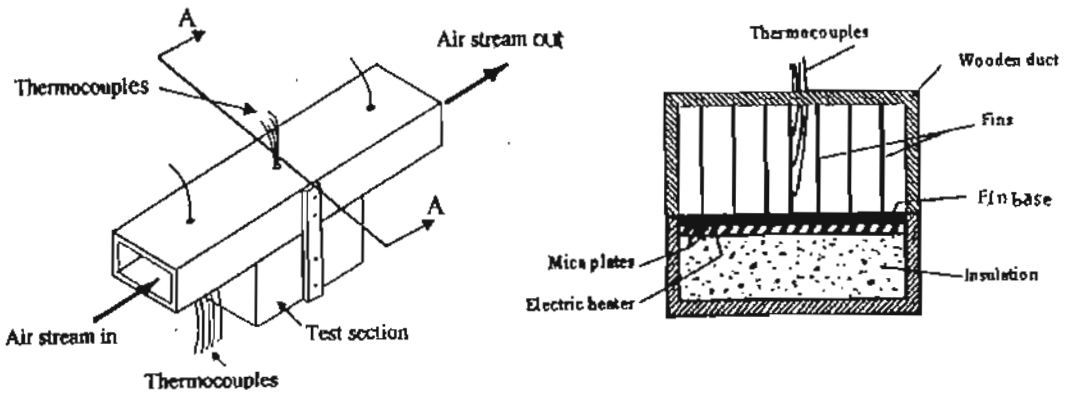

(a) (b)

Fig. 2. Test Section, (a) view of the test section, (b) cross sectional view at AA

The fin/base plate assembly is fabricated from aluminum for its high thermal conductivity and low emissivity. An electrical resistance wire, which served

to heat the fin array is sandwiched between two mica sheets and placed in contact underneath of the base plate and all the fin array assembly is then fitted into a wooden box filled with polystyrene insulation. The heat source is completely insulated on all sides in order to direct all heat to the fin array.

The closure of the fin gaps flow passages surrounded by an insulated U-shaped cross section wooden shroud with adjustable top, is attached to the fin array base plate at its outboard edges and sealed. This helps to minimize heat loss by conduction from the base plate to the shroud and prevent air leakage. The entire test section is insulated with glass wool sheet to minimize the heat loss.

As illustrated in Fig. 2-b, the assembly of the tested fin array when fully shrouded and of 7 longitudinal fins with 6 parallel flow passages bounded by half width fin spacing between the end side fins and the shroud.

The wind tunnel is run in suction mode. Air is drawn from the laboratory through its developing length, and then passed a calibrated velocity meter into the test section. From there, the air is sucked through a rectangular cross section duct by a centrifugal fan followed by a control air flow gate.

Heating Process and Instrumentation

The electric power is supplied to the heater by a regulated AC source via an autotransformer to control the voltage. The voltage settings are guided by the readings of thermocouples, and both the voltage drop and the current are measured by Voltmeter and Ammeter respectively.

Nine T-type thermocouples, 0.5 mm diameter, are glued onto to the base of the fin array, in nine 1.5 mm diameter drilled holes in the bottom surface of the base plate. Another six thermocouples are positioned along the longitudinal length of the middle fin, three at the mid half of its height and the other three at its tip. The bulk air temperature is detected by averaging of the readings of two thermocouples inserted upstream and that of another two thermocouples inserted downstream of the test section respectively. Temperatures are recorded by connecting the ends of all thermocouples via a selector switch to a 6 channels digital temperature recorder of 0.1 $^{\circ}$C resolution and with an accuracy of $\pm$ 0.5 $^{\circ}$C.

The air flow rate is controlled by the graduated gate located at the wind tunnel exit. A calibrated digital hot wire anemometer with a range of 0.2-20 m/s, a resolution of 0.1 m/s, , and an accuracy of $\pm$ (1%+ 1d) full scale respectively is used to measure the average velocity of entering air with the help of a traversing mechanism located 150 mm ahead of the test section. Two static pressure taps are located 100 mm ahead and down stream of the test section and connected to a U-tube water manometer for the measurements of the pressure drop across the fin array assembly.

The Test Matrix

The ducted fin array assembly is shown in Fig. 3. The clearance between the fin tips and the shroud which is represented by the top of the housing case is existed in practice such as in cooling of electronic components. When a clearance is present, the longitudinal flow tends to leak out of the fin passages where the flow resistance is low. The velocity distribution becomes more complex than for the no-clearance, as well as the heat transfer process.

In the present investigation, the height of the fins is held constant and the clearance between fin tips and the top of the test section can be varied by wooden smooth spacers with variable thickness that can be placed between the walls of the duct and the wooden shroud. The dimensional values of the fin array

assembly used in the study are summarized in Table 1.

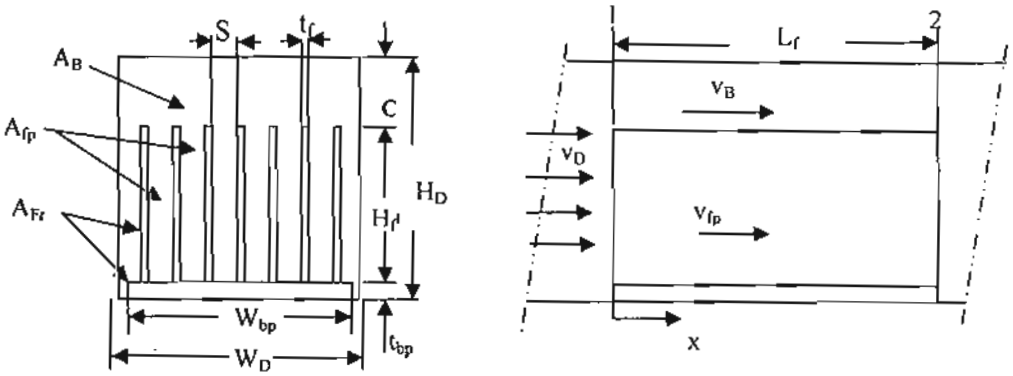

Fig. 3. Ducted fin array and by pass flow geometry

Table1: Geometrical parameters of the tested fin array.

Parameter	Range **Modeled**
Array material, Aluminum	k_f =237**W/m.K**
Number of fins, N_f	7
Base plate thickness, t_{bp}	3 mm
Bas plate, fin array width, W_{bp}	108 mm
Base plate length, L_{bp}	225 mm
Fin length, L_f	225 mm
Fin height, H_f	51 mm
Fin thickness, t_f	2 mm
Fin spacing, S	15 mm
Duct width, W_D	125 mm
Clearance, C	0,11.4,18.7, 28.6, 45.4 mm
Clearance ratio, C/H_f	0, 0.22, 0.36, 0.56, 0.89
Clearance ratio, C/S	0, 0.76, 1.25, 1.9, 3.0
Duct height, H_D	51,62.4,69.7,79.6,96.4 mm

Heat transfer and pressure drop results are parameterized by conventional rectangular duct Reynolds number, defined as

$$\mathrm{Re}=\frac{v_D\, D_h}{\nu} \qquad (1)$$

Where v_D is the duct air velocity upstream of the fin array and D_h is the hydraulic diameter of the fin array, given by

$$D_h=\frac{4A_F}{p} \qquad (2)$$

Where A_F is the free flow area and p is the wetted perimeter of the whole fin array assembly, expressed as

$$A_F=(W_D-N_f t_f)H_f+W_D C-W_{bp} t_{bp} \qquad (3),$$

$$p=2\left[(N_f+1)H_f+C+W_D\right] \qquad (4)$$

The fin array was installed in its position inside the test section and tested for two different power inputs, 75 W, and 100 W, at various air flow rates in terms of Reynolds number.

To attain a steady state condition, the system was initially run for about two to three hour until constant values of the recorded temperatures for both the bulk air and the array surface were observed.

Bypass Flow and Pressure Drop Analysis

The tested fin array is installed in the test section within the rectangular cross sectional duct as shown in Fig. 3. There will be a certain amount of flow bypasses and the velocity through the fin passages is different from the duct velocity approaching the fin array. The amount of bypass flow is related to the cross section geometry and the pressure drop across the fin array passages.

Considering the geometry shown in Fig. 3, and applying momentum and mass balances over the control surfaces 1 and 2, the total pressure drop across the fin array

as well as the by pass passages, Δp_t which is mainly consists of the pressure drop across the each passage due to friction and that due to the entrance and exit effects. This pressure drop is given by

$$\Delta P_t = \Delta P_{fp_f} + \frac{1}{2} K_{fp_{en}} \rho v_{fp}^2 + \frac{1}{2} K_{fp_{ex}} \rho v_{fp}^2 \quad (5),$$

$$\Delta P_t = \Delta P_{B_f} + \frac{1}{2} K_{B_{en}} \rho v_B^2 + \frac{1}{2} K_{B_{ex}} \rho v_B^2 \quad (6)$$

where ΔP_{fp_f} and ΔP_{B_f} are the pressure drop across the fin array and by pass passages due to friction, and K_{en} , K_{ex} are the entrance and exit loss coefficients for both the fin array and by pass passages geometries respectively. These coefficients [Kays and London, 1984] are given by

$$K_{fp_{en}} = 0.42\left(\frac{A_{fp}}{A_D}\right)^2 \quad (7),$$

$$K_{fp_{ex}} = \left(1 - \left(\frac{A_{fp}}{A_D}\right)^2\right)^2 \quad (8),$$

$$K_{B_{en}} = 0.42\left(\frac{A_B}{A_D}\right)^2 \quad (9),$$

and

$$K_{B_{ex}} = \left(1 - \left(\frac{A_B}{A_D}\right)^2\right)^2 \quad (10)$$

Substituting equation (5) into equation (6) gives

$$v_B^2 = \frac{\frac{f_{fp} L_{fp}}{D_{h_{fp}}} + K_{fp_{en}} + K_{fp_{ex}}}{\frac{f_B L_B}{D_{h_B}} + K_{B_{en}} + K_{B_{ex}}} v_{fp}^2 \quad (11)$$

Applying the continuity equation across the control surfaces, thus

$$v_B = \frac{v_D A_D - v_{fp} A_{fp}}{A_B} \quad (12)$$

where A_D is the duct cross sectional area approaching the fin array $(W_D \times H_D)$, expressed as

$$A_D = A_B + A_{fp} + A_{Fr} \quad (13),$$

A_B is the flow by pass area $(W_D \times C)$, A_{fp} is the flow area between fin array passages $(W_D - N_f t_f)H_f$, and A_{Fr} $(N_f H_f t_f + W_{bp} t_{bp})$ is the frontal area of the fin array.

Substituting equation (12) into equation (11), the flow velocity through the fin array passages (v_{fp}) can be described as a function of the duct flow velocity approaching the fin array (v_D) as follows

$$v_{fp} = \frac{-b \pm \sqrt{b^2 - 4ac}}{2a} \quad (14)$$

where

$$a = \left(\frac{A_{fp}}{A_B}\right)^2 - \frac{\frac{f_{fp} L_{fp}}{D_{h_{fp}}} + K_{fp_{en}} + K_{fp_{ex}}}{\frac{f_B L_B}{D_{h_B}} + K_{B_{en}} + K_{B_{ex}}},$$

$$b = \frac{-2 A_D A_{fp} v_D}{A_B^2}, \quad c = \left(\frac{A_D}{A_B}\right)^2 v_D^2 ,$$

$$D_{h_{fp}} = \left(\frac{4(W_D - N_f t_f)H_f}{N_f(2H_f + S + t_f)}\right), \text{ and } D_{h_B} \text{ is equals to } \left(\frac{2W_D \times C}{W_D + C}\right) \text{ are the hydraulic diameters of the fin array and the bypass passages, respectively.}$$

The values of v_{fp} can be determined from equation (14), substituting the value of the duct velocity (v_D) with the assumption of preliminary values for the friction coefficients for both the fin array and by pass passages as a fully turbulent flow. The obtained value of v_{fp} is then